Aspergillus-derived β-glucan nanoparticles: a dual strategy for *Fusarium Wilt* management and tomato plant growth enhancement

Parthasarathy Ramalingam[1,2]* and Manikandan Appu[3]

[1]Department of Biochemistry, Indian Institute of Science, Bengaluru, Karnataka, India, [2]Department of Biotechnology, RVS Agricultural College, Thanjavur, Tamil Nadu, India, [3]Department of Plant Sciences, University of Hyderabad, Hyderabad, Telangana, India

Introduction: A soilborne Ascomycete, *Fusarium oxysporum f.sp. lycopersicum*, is the causative agent of wilt disease, posing a significant threat to tomato plants and severely impacting global tomato production. Chemical fungicides are the primary strategy for controlling it. Employing fungicides arbitrarily and in huge dosages can pollute the environment and harm field workers and customers.

Methods: To combat tomato wilt, we synthesized β-glucan (isolated from the marine algal associate *Aspergillus awamori*) nanoparticles (β-glu-n) and evaluated their efficacy in promoting plant growth and suppressing *Fusarium oxysporum*.

Results and discussion: The synthesized β-glu-n was confirmed using NMR and IR spectroscopy. The spherical shape with a smooth surface and average size of 35 ± 6.0 nm was observed by TEM. The hydrostatic zeta potential was -38.40 mV, indicating colloidal stability. The crystalline structure of the β-glu-n was confirmed by the XRD spectrum. Furthermore, a significant seed germination and growth profile, including higher shoot and root length and lateral root, was observed in the β-glu-n-treated tomato seeds count than in the mycelial glucan (m-β-glu) and control group under glasshouse conditions. Moreover, novel protein polypeptides were derived from β-glu-n-treated plants, indicating the increased photosynthetic rate. β-glu-n inhibited *Fusarium oxysporum* in a disc diffusion test and reduced wilt symptoms in under detached leaf assay. These results suggest that β-glucan nanoparticles can promote plant growth and prevent tomato wilt disease.

KEYWORDS

Aspergillus awamori, β-glucan nanoparticles, tomato wilt, *Fusarium oxysporum*, detached leaf assay

1 Introduction

Tomatoes (*Solanum lycopersicum L.*) rank among the most favoured fruits globally and widely consumed vegetables, noted for their nutritional value and economic importance (Quinet et al., 2019; Erika et al., 2020). Their tomato yield was decreasing due to the crops being impacted by the wilt disease, caused by the *Fusarium oxysporum f.sp. lycopersicum* (soil-borne pathogen). This pathogen enters tomato plants through their roots all the growth level stages, producing significant economic losses by causing necrosis and wilting, eventually culminating plant death. Controlling this pathogen remains tough due to its long-term stay in the soil and capacity to infect a large number of host plants (Jangir et al., 2021; El-Aswad et al., 2023; Chakrapani et al., 2023);.

Therefore, it is crucial to investigate an effective and environmentally friendly alternative, offered the considerable interest in biological control agents. These methods control these pathogens through natural bio-resource or bio-based polymers and provides benefits including availability from sustainable agricultural resources, biodegradable properties and ecological safety, which can enhance the plant defense mechanisms. β-glucans are the primary polysaccharides in the cell wall that play a crucial role in inducing systemic resistance (defense mechanism) during pathogen infection (Camilli et al., 2018). It has also been demonstrated that it improves crop protection against pathogens and enhances plant growth development (Riseh et al., 2023; Chavanke et al., 2022).

The emergence of nanotechnology and the advancement of innovative nanomaterials explore potential openings and new applications in agricultural biotechnology (Iavicoli et al., 2017; Shang et al., 2019; Sundararajan et al., 2023). β-glucan nanoparticles have widespread applications in different areas, used as drug delivery systems (Huang et al., 2020), anticancer molecules (Parthasarathy et al., 2021) and biocontrol agents, biofertilizers (Murphy et al., 2022). Their nanoscale dimensions improve bioavailability and surface reactivity, rendering them effective in targeting phytopathogens (Chavanke et al., 2022). Moreover, biopolymer-based nanoparticles, such as glucan and chitosan, have the capacity to improve plant growth development by enhancing nutrient uptake and optimizing photosynthate effectiveness (Photosynthesis) and also inhibiting fungal pathogens specifically, β-glucans nanoparticle can stimulate the activities of key enzyme such as peroxidase and polyphenol oxidases, which are associated with both defence and metabolic efficiency there by potentially enhancing the allocation and utilization of photosynthates rates for plant growth and development (Kaziem et al., 2024; Melo et al., 2020). Recently, Anusuya and Parthasarathy (2025) reported that glucan nanoparticles were synthesised using sodium tripolyphosphate have much attention for their biocompatibility and biocidal properties.

The current study focuses on the preparation of nanoparticles derived from fungal glucan, extracted from the marine algal associated fungi. It determines their effectiveness against wilt disease caused by *Fusarium oxysporum f.sp. lycopersicum* and their capacity to stimulate the growth of tomato plants. The purpose of this research is to modify bio-resources into nanocomposites to provide an effective and eco-friendly method for protection against pathogens and to enhance the growth and development of tomato plants.

2 Materials and methods

2.1 Pathogen and seeds collection

Tomato wilt pathogen (*Fusarium oxysporum*) was obtained from the Indian Type Culture Collection (ITCC), Indian Agricultural Cultural Research Institute (IARI), New Delhi, India. The pathogen was maintained at 4°C.

Tomato seeds of the PKM-1 variety were received from Tamil Nadu Agricultural University (TNAU), Coimbatore, Tamil Nadu, India.

2.2 Collection and transport of *Ulva lactuca*

Ulva lactuca (marine green algae) was obtained from the shoreline of Rameswaram, Tamil Nadu, India. Fresh and healthy thalli were carefully handpicked and immediately placed in sterile polythene bags filled with seawater to maintain their physiological condition and prevent dryness. The collected algae samples were carried to the laboratory within 24 hours of collection for endophytic fungi isolation.

2.3 Fungal material: isolation and identification

The endophytic fungus was isolated and identified following the method described by earlier reports (Parthasarathy and Sathiyabama, 2014; Parthasarathy et al., 2020). In brief, the fungus was obtained from the marine green algae *Ulva lactuca*. The isolated fungal strain (designated as UL) was cultured on potato dextrose agar (PDA) medium supplemented with sea salts, adjusted to pH 5.1. The cultures were incubated at 30°C for a period of 10-15 days. By the 10th day of incubation, the fungus developed black and white colonies on the surface of the PDA medium (Supplementary Figure S1).

Fungal genomic DNA was isolated to enable molecular characterization of the species. The ITS region was targeted for amplification using ITS 1 as the forward primer and ITS 4 as the reverse primer. The resulting amplified ITS product was sequenced and analysed for species identification using the BLAST tool. The analysis revealed a 99% identity with *Aspergillus awamori* (AA). The sequence was subsequently deposited in the NCBI GENBANK database and assigned the accession number MH920241.1 for the fungal species. Additionally, a phylogenetic tree based on the ITS sequence of *A. awamori* was constructed using the neighbor-joining method. The analysis demonstrated a 99.5% similarity to other *A. awamori* species, further confirming the identity of the isolate (Supplementary Figure S2).

2.4 Extraction of glucan from fungal mycelium

A. awamori spores ($1x10^5$/mL) were inoculated into potato dextrose broth (PDB) and incubated for 7 days at 27°C. Then, the fungal mycelium was harvested and washed with sterile distilled water. The mycelia were then resuspended in double distilled water (10 mL/g mycelium) and pulverized using a pestle and mortar. The mycelial slurry was filtered through filter paper. The residue was homogenized three times in water, once in a 1:1 combination of chloroform and methanol, and finally in acetone before being dried at 55°C using a rotary vacuum evaporator. The mycelial wall was pulverized into a fine powder using a sterile pestle and mortar before being extracted with 100 mL of 1 M NaOH at 95°C for 2 hours to remove proteins, lipids, and alkali-soluble polysaccharides. The resulting suspension was subsequently allowed to reach room temperature, filtered, and then neutralized with the water. The pellet was rinsed with 95% ethanol (v/v) and freeze-dried. The dried powder was treated with 20% (v/v) HCl (50 ml/g dry matter) overnight at 60°C and stirred. The precipitate was neutralized with distilled water, freeze-dried, and kept at 4°C to prepare nanoparticles (Anusuya and Sathiyabama, 2014; Sathiyabama and Charles, 2015).

2.5 Synthesis of glucan nanoparticle from mycelial glucan

1 g of mycelial glucan (m-glu) was dissolved in 100 ml of 2% NaOH (w/v) while maintain controlled magnetic stirring for 3 hours at 90°C. At the end of incubation period, β-glucan nanoparticles (β-glu-n) were precipitated using 1% (v/v) acetic acid. To prepare a stable suspension of 5mg/mL β-glu-n, the solution was added dropwise to a tripolyphosphate (2mg/mL) solution while stirring magnetically at room temperature. The suspension was then stirred for an additional hour at room temperature before being centrifuged at 5000 rpm for 20 minutes. The pellet was washed with MilliQ water to remove debris and stored at 4°C for characterization and bioactivity assessment (Parthasarathy et al., 2021).

2.6 NMR analysis of mycelial β-glucan and β-glucan nanoparticles

The m-β-glu and β-glu-n were analyzed using NMR to confirm the β glucan and its nano-reductant. The m-glu and β-glu-n (5mg) were dissolved in DMSO-D6and transferred to an NMR glass tube associated with the NMR JEOL apparatus. The 500 MHz spectrometer was employed to acquire Nodel ECZ500 spectra at a stable temperature of 80°C. The ^{1}H NMR spectra were obtained within a scan range of 2000 (0-7 ppm).

2.7 IR spectrum analysis of β-glu-n

The prepared m-β-glu and β-glu-n were ground into fine powders and mixed with KBr to form pellets. The pellets underwent analysis with a Thermo-Nicolet 6700 FTIR spectrophotometer, covering the infrared range of 400-4000 cm^{-1}.

2.8 Ultraviolet spectral analysis of β-glu-n

The SPR (surface plasmon resonance) of β-glu-n was measured using a UV-Vis spectrometer (J Shimadzu MPC3600) at 200-500 nm.

2.9 Assessment of size and zeta potential for β-glu-n

The β-glu-n was dissolved in deionized water and subsequently transferred into a glass cuvette, where it was positioned on the ZETA PALS. The temperature remained constant at 25°C throughout the entire process. The sizes of nanoparticles and their distribution range were recorded, as well as the values for the polydispersity index (PDI) were measured.

2.9.1 HR-TEM and SEM analysis of β-glu-n

The morphology and size of β-glu-n were assessed using a scanning electron microscope (FEI ESEM QUANTA 200) and transmission electron microscopy (TEM). Desiccated β-glu-n were positioned on the copper grid of the Titan Themis 300 kV FEI Transmission Electron Microscope (ULTRA 55-GEMINI technology). The size, structure, and micrograph of the nanoparticles were captured.

2.9.2 X-ray diffraction pattern of β-glu-n

The dried β-glu-n were placed on a glass slide, and the sample was analyzed using the Rigaku Smart Lab general-purpose X-ray diffractometer system (utilizing XPERT Pro, PANalytical JDX-8030, and JEOL). The diffraction intensities of the nanoparticles were measured across a 2θ angle range from 10 to 90°.

2.9.3 Invitro assessment of β-glu-n on *F.oxysporum* growth

In Vitro assessment of β-glu-n *F. oxysporum* inhibition potential was assessed on PDA plates using the disc diffusion method. β-glu-n and m-glu were dissolved in sterile distilled water (100μg/mL). Five-day-old *F.oxysporum* mycelial plugs (6-mm-dm) were placed on a PDA plate. A sterile disc (5mm-dm) loaded with β-glu-n (50μl) and m-glu (50μl) was placed alongside the *F. oxysporum* culture and incubated at 24°C for 48 hours. The disc with sterile distilled water was employed as a control.

2.9.4 Efficacy of β-glu-n on disease development assessed using detached leaves assay

The effectiveness of β-glu-n in controlling *F. oxysporum*-induced wilt disease in tomato plants was examined using the detached leaves assay (Manikandan and Sathiyabama, 2016). To do this, 25-day-old tomato leaves were carefully plucked off the plants with sterile blades. The leaves were cleaned adequately with running tap water to remove debris, followed by two washes with sterile distilled water *in vitro*. Following sterilization, the leaves were placed in petri dishes and covered with filter paper for 5 minutes to remove excess moisture. Sterilized leaves were treated with 0.1% (w/v) β-glu-n and m-glu (50 µl/leaf) using a sterile acrylic brush and 5 ml of sterile distilled water were treated as a control. The leaves were incubated at $25 \pm 2°C$ for 24 hours. After 24 hours, treated and control leaves were challenged with a spore suspension of *F. oxysporum* (1×10^5 spores/ml) (100 µl/leaf) applied with a sterile acrylic brush. To assess disease progression, treatment and control leaves were kept at $25 \pm 2°C$ and 100% humidity for 15 days.

2.9.5 The effect of β-glu-n on plant development in a greenhouse environment

Tomato seeds treated with 5ml of 0.1% (w/v) β-glu-n and m-glu were placed in poly plant growing bags (12 x 12 inches) containing soil, and infected with spores of *F. oxysporum* (1×10 spores' ml^{-1}) in a greenhouse environment. Tomato plants grown in soil with solely *F. oxysporum* spores (1×10 spores' ml^{-1}) served as the control group. Growth profiles including shoot length, root length, and leaf count were meticulously recorded in both treated and control plants. Each experiment utilized 50 plants, with three repeats performed.

2.9.6 Implications of β-glu-n on protein profile in tomato leaves

The treated and control tomato leaves were collected on 25th day. Leaves were homogenised in 0.02 M sodium acetate buffer and centrifuged at 10,000 rpm for 20 minutes at 4°C. The protein content in the supernatant was determined using the Bradford method (Bradford, 1976). The samples (30 µg) underwent denaturation for five minutes in a boiling water bath with SDS and sample buffer, followed by separation with marker proteins (Bradford, 1976). The localization of polypeptides on SDS PAGE was achieved through staining with Coomassie Brilliant Blue.

3 Results and discussion

Continuous innovation in agriculture is necessary to address present obstacles including food security, and climate change. This expands scope of nanotechnology as a new source for improving existing crop management techniques (Shang et al., 2019; Ahmad et al., 2024). The use of nanomaterials, particularly those based on natural source is becoming more popular due to their high specificity and improved functionality, and typically excellent biocompatibility. Glucan nanoparticles, in particular are valued for their consistent structure and widely applied in fields including drug delivery and the agricultural sector (Kaziem et al., 2022; Chen et al., 2024).

3.1 Characterization of β-glucan nanoparticles

This research focused on the synthesis of mycelial glucan nanoparticles via biological method using sodium tripolyphosphate (TPP). A total of 15 g of mycelial β-glucan was extracted from *A. awamori*. Additionally, the synthesis of β-glu-n, specifically mycelial glucan, was achieved by solubilizing in NaOH at ambient conditions. The resulting nanoparticles were formed through electrostatic interaction between the glucan and tripolyphosphate (TPP), with their shape, structural uniformity and stability being influenced by these interactions.

The typical 1H NMR chemical shifts for carbohydrate ring proton range from 3-6 ppm. The synthesis of β-glu-n was corroborated by 1H NMR signals corresponding to m-β-glu (4.35,4.58) and β-glu-n (4.50,4.68 ppm), which indicated of β-1,6 linkages (Figures 1a, b). A signal at 3.39ppm appeared exclusively for nanoparticles and was ascribed to the H-1 phosphate connected to the α-anomer at the reducing end. These 1H signals assignments align with values previously documented values for analogous compounds (Kim et al., 2000; Parthasarathy et al., 2021).

The IR spectrum of β-glucan exhibited a characteristic pattern typical of carbohydrate moieties, with several bands observed in the anomeric area. The β-glu-n and m-glu IR spectra displayed a distinctive absorption peak at 892.67 and 893.34 cm^{-1}, respectively, indicative of β-glucan (Figure 2a). Moreover, m-glu and β-glu-n peaks were observed at 2921.45, 1374.51, 1148.67, 1042.32 cm^{-1}, and 1329.10, 1162.31, 1162.31,1034.78 respectively, signifying β-(1-3) linkage. The β-glu-n was changed through the regulated incorporation of TPP, which conferred structural integrity and stability to the nanoparticles. A peak at 2508.63 cm^{-1}, resulting from the OH-P=O stretch, can be ascribed to the connection between the phosphoric group of TPP and the CH_2OH group of the β glu-n (Figure 2b) (Limberger-Bayer et al., 2014; Bacha et al., 2017; Mahmoud and Yassein, 2024)

The UV-visible spectrum exhibited a prominent surface plasmon resonance (SPR) peak at 389.45 nm, confirming the synthesis of β-glu-n stabilized at ambient temperature (Supplementary Figure S3).

DLS demonstrated the average size of the β-glu-n in the range of 85.3 nm, with a narrow size distribution and strong dispersion (Polydispersity Index of 0.284) (Figure 3a). The zeta potential was -38.40 mV, demonstrating colloidal dispersion of the nanoparticles (Figure 3b). The detrimental impact could be due to TPP binding, which produces repellent effects on nanostructures (Wu et al., 2005; Khlebtsov and Khlebtsov, 2011). The low index of polydispersity indicates a uniform size range of the nanoparticles, reflecting effective fabrication and stability. This results in particles that are less prone to aggregation and demonstrate consistent behaviour in different conditions (Ashraf et al., 2021).

HR-TEM images showed a uniform arrangement of β-glu-n, with an average size of 35 ± 6.0 nm (Figures 4a, b). The β-glu-n exhibited a colloidal nature, which was indicated by a spherical

FIGURE 1
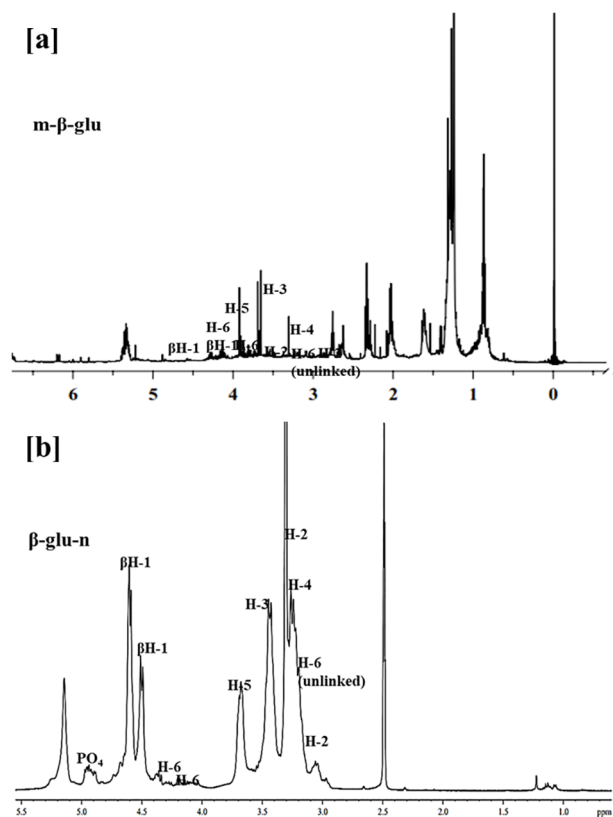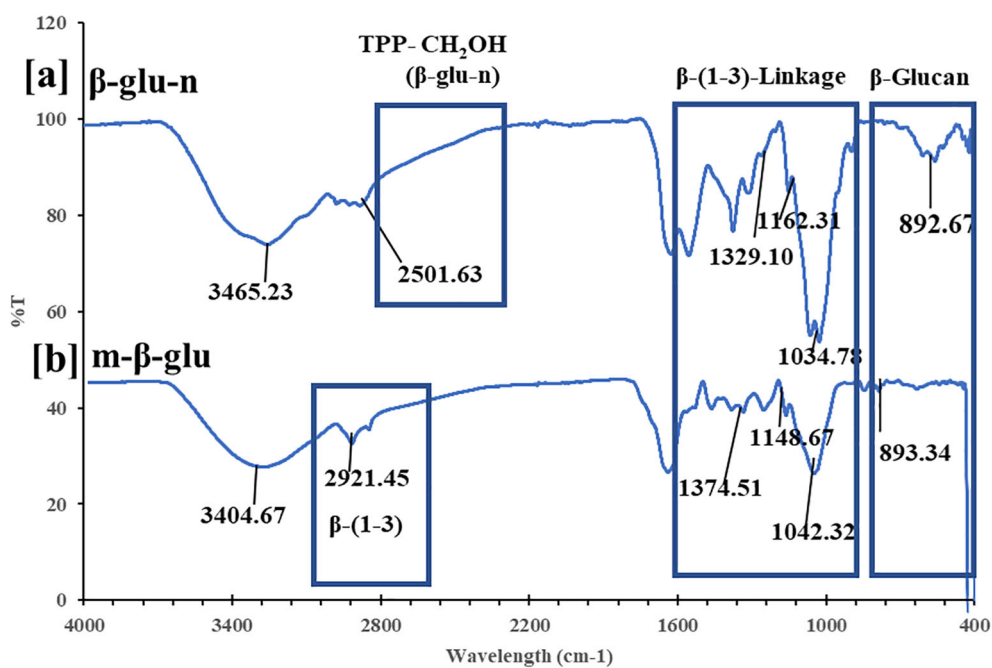(a, b) ^{1}H NMR spectrum of (a) m-β-glu (b) synthesized β-glu-n with tripolyphosphate (TPP).

FIGURE 2
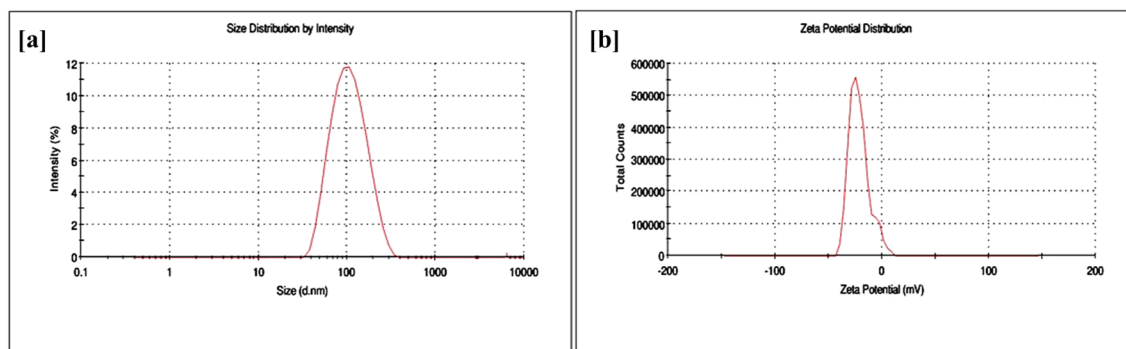(a, b) IR spectrum analysis of (a) β-glu-n (b) m-β-glu.

FIGURE 3
(a, b) Particle size **(a)** and zeta potential **(b)** analysis of β-glu-n.

shape and a smooth surface, revealing long-term durability. The SEM images also displayed a round morphology with a smooth surface (Figure 4c). Both SEM and TEM demonstrated an even distribution of nanoparticles, primarily attributed to the presence of TPP in the synthesis process (Piani and Papo, 2013). The HR-TEM and DLS size of the nanomaterials exhibited variance due to the different principle and concepts involved. The synthesized glucan nanoparticles underwent modification through the controlled addition of TPP, enhancing their structural integrity and stability.

The X-ray diffraction (XRD) analysis of β-glu-n depicted prominent diffraction peaks at 22θ = 25.06°, 32.3°, and 42.1° (Figure 5). These peaks are indicative of the crystalline nature of the β-glu-n, aligning with characteristics patterns previously studies for polysaccharides-based nanoparticles. Such crystalline features are commonly observed in β-glucan, as reported previous study (Elnagar et al., 2021).

3.2 Assessment of β-glu-n action on tomato wilt (*F. oxysporum*) disease

The *in vitro* mycelial growth of *F. oxysporum* significant inhibition when treated with β-glu-n at a concentration of 50 μL. β-glu-n demonstrates a remarkable ability to inhibit the growth of *F. oxysporum* by 92.67%, while the mycelial glucan exhibits an average inhibition rate of 62.35%. No inhibition was noted in the control plates. (Figure 6). The results demonstrated that β-glu-n showed enhanced effectiveness against *F. oxysporum* under *in vitro* conditions. The presence of positively charged β-glucan molecules could be a contributing factor, as their interaction with negatively charged membranes appears to be one of the potential mechanisms involved. Previous studies suggested that the compact structure of β-glu-n may facilitate its passage through fungal cell walls, allowing it to attach to DNA and proteins, potentially hindering DNA replication,
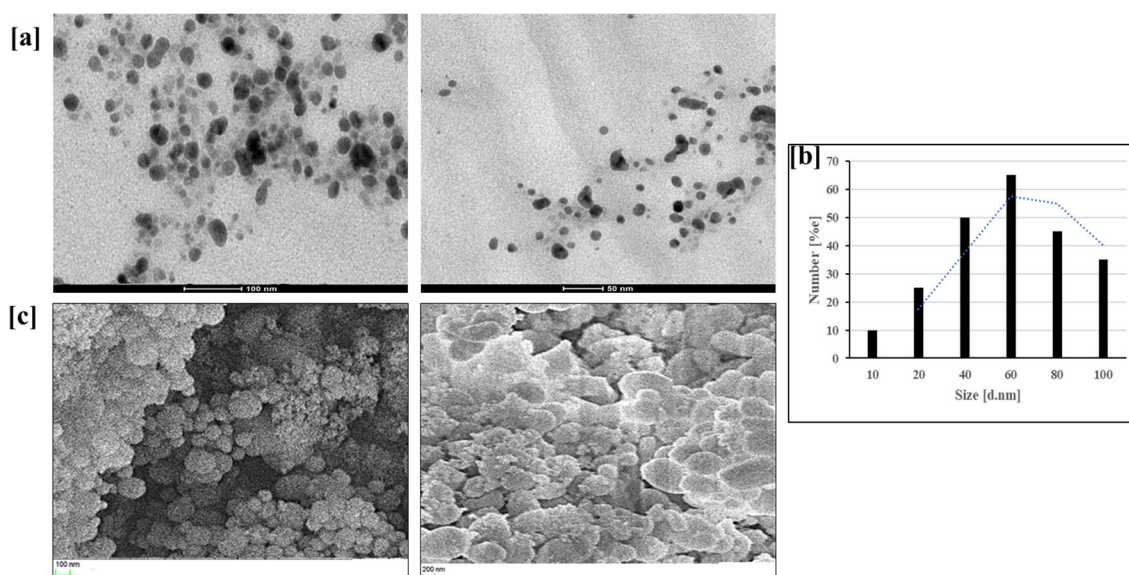
FIGURE 4
(a–c) HR-TEM images of β-glu-n **(a)**, particle size distribution histogram of β-glu-n **(b)**, SEM micrograph of β-glu-n **(c)**.
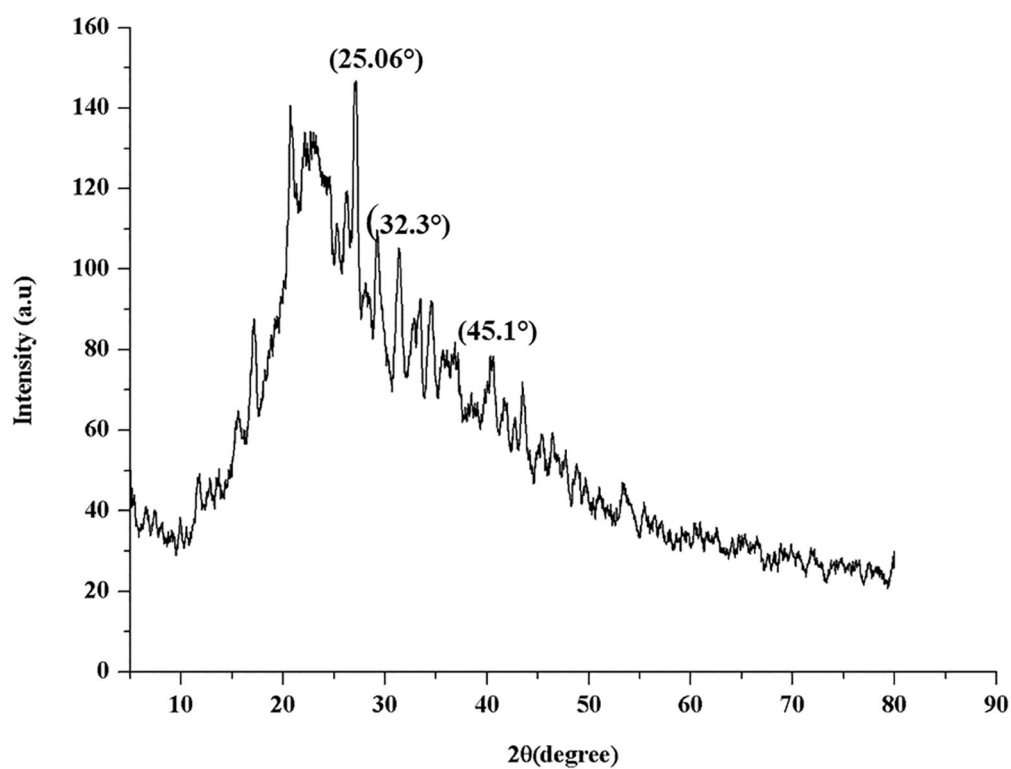
FIGURE 5
XRD analysis of β-glu-n.

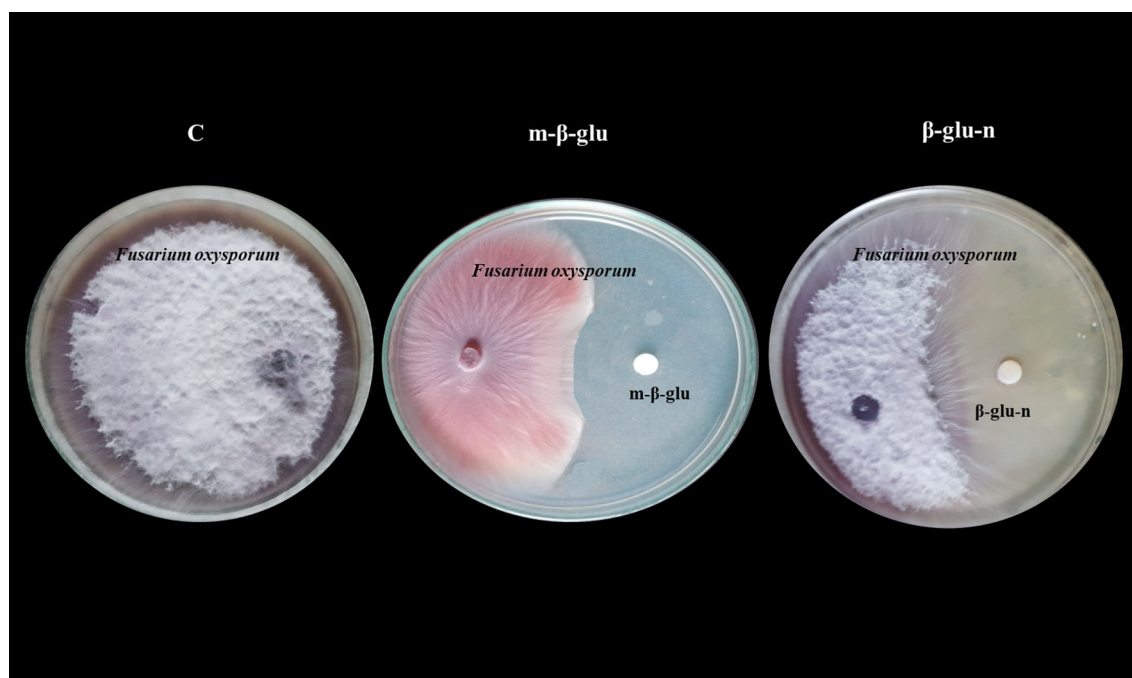
FIGURE 6
Inhibitory effect of m-β-glucan and β-glu-n on tomato wilt (*F. oxysporum*). C-Control- No Inhibitory effect, m-β-glu-62.35% growth inhibition.
β-glu-n-92.67% growth inhibition.

leading to cellular dysfunction and death. Moreover, the interaction with the cell wall can stimulate the production of reactive oxygen species (ROS) within the fungal cell further contributing to oxidative stress and cellular damage (Kamiński et al., 2022). This result aligns with previous studies indicating that β-glucan nanoparticles exhibit antifungal activity against the phytopathogen *P. aphanidermatum* (Anusuya and Sathiyabama, 2014).

The detached leaf techniques provide an *in vivo* environment for the interacting plant pathogens, resulting in effects comparable to those reported in whole plants (Chandra et al., 2015). Symptoms of wilt were observed in leaves treated with m-β-glu after 5 days of infection, with half of the leaf surface exhibiting disease by day 10. In the control group, the symptoms of the disease manifested after a period of two days. Additionally, the presence of the disease (100%) was evident after 15 days in the control group and continued to advance. Leaves that were treated with m-β-glu exhibited a reduction of over 50% in wilt disease in comparison to the untreated infected control. In leaves treated with β-glu-n, a total suppression of wilt disease was noted throughout the entire experimental period (Figures 7a–c). The results affirm the bioactive properties of β-glu-n. This study represents the first investigation of β-glu-n's ability to reduce wilt disease in tomato plants. Polysaccharide-based nanocomposites, including fungal cell wall glucan and chitosan, have the ability to infiltrate the plant tissues due to their small size, gaining entry through stomata,

wounds, trichomes, and various other points of access (Fernández and Eichert, 2009; Anusuya and Sathiyabama, 2014; Su et al., 2019). Stomata act as an important route for the absorption of nanomaterials (Ali et al., 2011; Ashok Kumar et al., 2014). Tomato plants have stomata on both surfaces (Henningsen et al., 2023), which may have enabled the rapid absorption of β-glu- n. Upon entering, it may trigger the immune response, thereby controlling the growth of invasive plant pathogens alongside with its bioactive properties (Fuertes-Rabanal et al., 2024). Additionally, the increased quantity of superficial functional structures found in β-glu-n enhances its interaction with plant cells.

3.3 Assessment of β-glu-n effect on tomato plant growth condition

The tomato seeds treated with β-glu-n and m-β-glu exhibited favourable morphological effects, including improved percentage of germination, increased root and shoot length, a higher seed vigor index, and more effectively vegetative growth of seedlings. Seeds treated with β-glu-n displayed a 100% germination rate and improved seed vigor index (2060), compared to 95% in m-β-glu with seed vigor index (2010) followed by the 85% in control group with a lower vigor index (1302) (Figure 8a). Figure 8b illustrates that seedlings treated with β-glu-n and m-β-glu exhibited notably longer
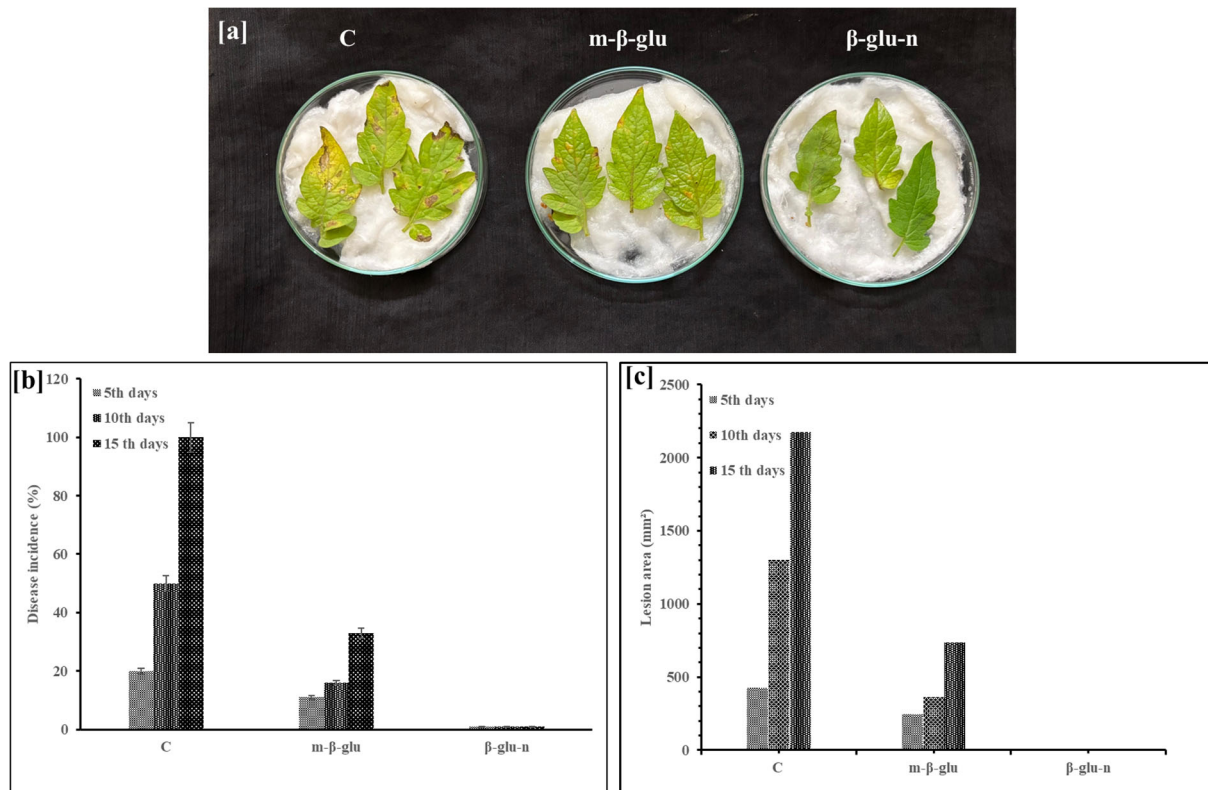
FIGURE 7
(a, b) Suppression of wilt disease on detached leaves of tomato plants. **(a)** C-Control - no suppression of wilt disease; m- β-glucan - 50% suppression of wilt disease; β-glu- n - total suppression of wilt disease. **(b)** Wilt disease incidence percentage on leaves observed on the 5th, 10th, and 15th days for control, m-β-glu, and β-glu- n. **(c)** Symptoms of wilt disease in the lesion area (mm^2) 5, 10, and 15th day control, m-β-glu, and β-glucan- n.

FIGURE 8
(a, b) Effect of β-glu-n on seed germination (%), mean shoot length (cm), mean root length(cm), seedling length and number of lateral roots in tomato plants (a). Effect of β-glu-n and m- β-glu on tomato seedling growth (b).

shoots and roots in comparison to the control group. Additionally, administering β-glu-n led to more lateral root growth in tomato seedlings. The results suggest the β-glu-n treatment d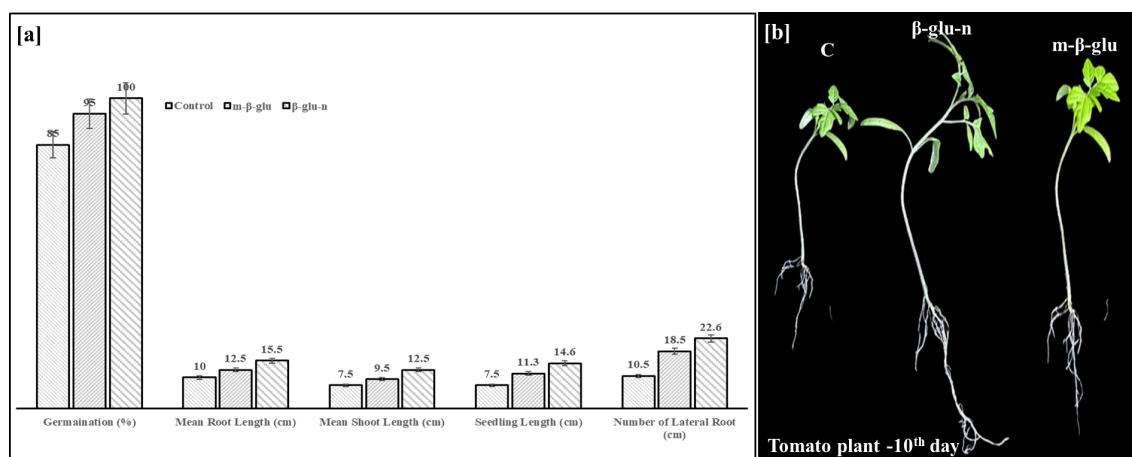emonstrated improved effectiveness in promoting tomato plant growth. Seeds treated with nanoparticles have demonstrated enhanced vigor and improved seedling development across various crops (Arruda et al., 2015). Ultimately, the β-glu-n treatment enhanced tomato plant growth significantly. β-glu-n is absorbed by seeds and transported during photosynthesis. Tan et al. (2012) reported that applying uniconazole-silica nanoparticles to *Oryza sativa* increased the number of roots, root length, and plant fresh weight. Exposure to nanoparticles resulted in increased shoot length as well as a greater growth rate in root tissue, demonstrating an improvement in lateral root growth when compared to the control group. Root lengthening acts as a more precise indicator for assessing the phytotoxic impacts of nanotechnology (EI-Temsah and Joner, 2012). At a root plane, the connections of the rhizoderm is and lateral roots may enable access to nanomaterials, particularly near the root tip, while the upper regions stay impermeable due to the deposition of suberin on the outer layer (Chichiriccò and Poma, 2015). Additionally, the negatively charged nanoparticles are swiftly transported to the bottom of the essential cylinder, enabling their ascent to the plant's aerial part (Avellan et al., 2017; Zhao et al., 2017).

In evaluating the growth of tomato plants, those treated with β-glu-n and m-β-glu exhibited enhanced growth in plant growing bags, showing no adverse effects, whereas control plants exhbits the leaf lesion symptoms with decreased growth (Figure 9). Chemical fungicides, along with metal or carbon-based nanoparticles, were utilized in the soil as fertilizers for agricultural plants (Gao et al., 2006; Verma et al., 2018). Considering the significant evidence, the use of nanoparticles and chemical fungicides as soil additives may present a threat to soil microbes, consequently limiting the application of metallic nanoparticles in agriculture practices (Simonin et al., 2016; Goncalves et al., 2017). Biopolymer/natural nanocomposites are regarded as significantly less harmful because of the slow-release phenomena, and their enduring impact has been

evidenced in agricultural crop plants. The use of glucan-based nanocomposites in agricultural crops improves the length of leaves, shoots, and roots (Anusuya and Sathiyabama, 2014). The treatment with glucan nanocomposite may have increased levels of gibberellic acid, which play a key role in shoot development (Stepanova et al., 2007). Glucan nanoparticles administration likely interacts with ethylene inhibition, leading to a reduction in abscission occurrence. This interaction significantly contributes to the observed increase in leaf number (Seif et al., 2011).

3.4 Examination of the protein profile in β-glu-n-treated tomato plants' growth

The leaves of the treated (β-glu-n and m-β-glu) crops exhibited an increase protein content when compared to the control (Figure 10a). Electrophoresis was utilized to assess ribulose bisphosphate carboxylase (Rubisco), a crucial enzyme in the process of photosynthesis (Aranjuelo et al., 2005). The SDS-PAGE analysis of the protein in the tomato leaves on the 25th day showed that both the control and treated tomato plants displayed polypeptides ranging from 25 to 90 kDa comparison with standard protein marker. Furthermore, the β-glu-n treated tomato plants leave exhibited the presence of three novel polypeptides with molecular mass of 14, 19, and 23 kDa. The treated (β-glu-n and m-β-glu) seedlings exhibited elevated levels of a molecular mass of 54.5 kDa when compared to the control group (without treatment). (Figure 10b). The structure comprises two major subunits, each with a weight ranging from 50 to 55 kDa, in addition to two smaller subunits that range from 12 to 18 kDa. The combined components could account for roughly half of the total soluble protein and a quarter of the total nitrogen present in leaf tissue (Tabita et al., 2007). The function of Rubisco is to boost the overall photosynthetic efficiency of cereal crops in various climates (Parthasarathy et al., 2023). Nitrogen-courting rice and Rubisco have demonstrated their ability to improve the crop development

FIGURE 9
Effect of β-glu-n and m- β-glu on tomato plant growth development under glass house condition-control, β-glu-n and m- β-glu.

and leaf photosynthesis (Makino, 2003; Perdomo et al., 2017). Nanoparticles (NPs) influence Rubisco dynamics in dicot plants by delaying its natural degradation post -leaf maturation, thereby sustaining photosynthetic activity beyond typical growth phase. This effect is confirmed through electrophoretic analysis showing persistent Rubisco presence even 25 days after Nps exposures.

This research indicates that β-glu-n can be synthesized using TPP, demonstrating its potential applications in agriculture for enhancing plant growth and managing diseases.

Further studies are necessary to thoroughly assess the toxicity and safety considerations, molecular mechanism of biosynthesised β-glu-n before its widespread application in the agricultural sector. In addition, understanding the environmental fate and potential accumulation of β-glu-n in the ecosystem is crucial for developing safe and effective agricultural uses. Consequently, through safety

assessment and regulatory evaluations are essential steps prior to endorsing the large-scale use of biosynthesised β-glu-n in agricultural field.

4 Conclusion

To sum up, the investigation outlines the synthesis of β-glucan nanoparticles using TPP. The β-glucan extract is derived from the marine algal associate fungi (*A. awamori*) and confirmed via ^{1}H NMR. The structure of the β-glu-n was analyzed using ^{1}H NMR and IR spectrum. The glucan nanoparticles that were synthesized underwent characterization via HR-TEM, DLS, and XRD analyses. The zeta potential of the biosynthesized β-glu-n was measured at -38.40 mV, suggesting its colloidal stability in a water solution. β-

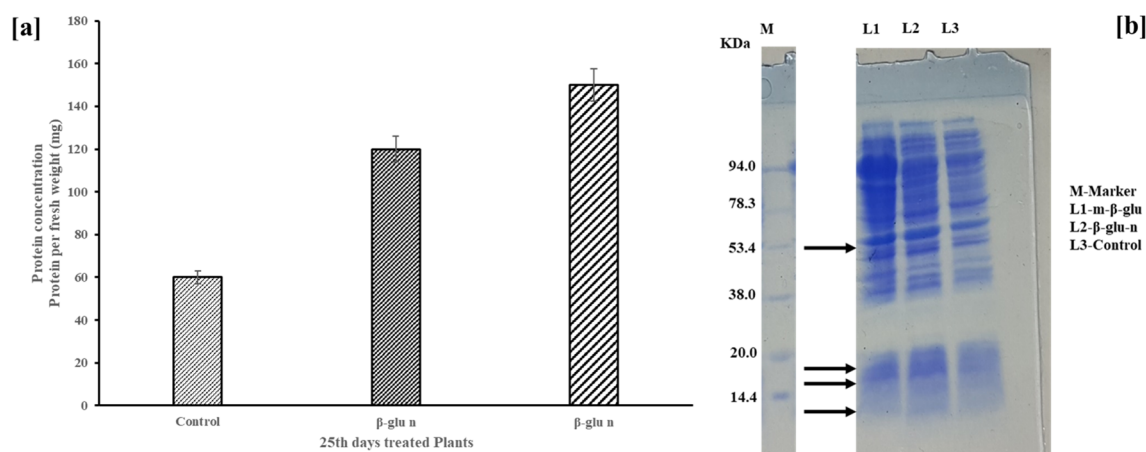**FIGURE 10**
(a, b) Protein levels of control, and treated (β-glu-n, m- β-glu-n) tomato plant leaves **(a)**, The SDS-PAGE analysis of the protein in the tomato leaves on the 25th day displayed M-Marker- standard protein marker, L1- β-glu-n, L2- m- β-glu, L3-Control **(b)**.

glu-n demonstrated inhibitory activity against the highly destructive tomato wilt pathogen *F. oxysporum* under *in vitro* conditions. The detached leaf method demonstrated suppression in wilt diseases in tomato leaves and indicates that β-glu-n may be effective in managing tomato pathogens, enhancing plant growth and protein content. Thus, this study demonstrates that β-glu-n, when used in crops seeds and fertilizer amendments, can enhance productivity in modern agriculture and serve as an innovative solution for tomato wilt disease. Additional research into the biochemical and molecular factors in field conditions is essential to confirm the precise mechanisms.

4.1 Statistical analysis

The data was analyzed using one-way ANOVA to determine the significance of individual differences at $p < 0.01$ and 0.05 levels. All statistical analyses were carried out using SPSS 21 software support version 5.0.

Data availability statement

The datasets presented in this study can be found in online repositories. The names of the repository/repositories and accession number(s) can be found in the article/Supplementary Material.

Author contributions

PR: Conceptualization, Data curation, Formal analysis, Investigation, Methodology, Project administration, Resources, Supervision, Validation, Writing – original draft, Writing – review & editing, Software, Visualization. MA: Formal analysis, Methodology, Writing – review & editing.

Conflict of interest

The authors declare that the research was conducted in the absence of any commercial or financial relationships that could be construed as a potential conflict of interest.

Generative AI statement

The author(s) declare that no Generative AI was used in the creation of this manuscript.

Publisher's note

All claims expressed in this article are solely those of the authors and do not necessarily represent those of their affiliated organizations, or those of the publisher, the editors and the reviewers. Any product that may be evaluated in this article, or claim that may be made by its manufacturer, is not guaranteed or endorsed by the publisher.

Supplementary material

The Supplementary Material for this article can be found online at: https://www.frontiersin.org/articles/10.3389/fpls.2025.1611582/full#supplementary-material

References

Ahmad, Z., Niyazi, S., Firdoos, A., Wang, C., Manzoor, M. A., Ramakrishnan, M., et al. (2024). Enhancing plant resilience: Nanotech solutions for sustainable agriculture. *Heliyon.* 10, e40735. doi: 10.1016/j

Ali, S. W., Rajendran, S., and Joshi, M. (2011). Synthesis and characterization of chitosan and silver loaded chitosan nanoparticles. *Carbohydr. Polym.* 83, 436–446. doi: 10.1016/j.carbpol.2010.08.004

Anusuya, S., and Parthasarathy, R. (2025). Natural synthesis of β-glucan nanoparticles via microwave for breast cancer prevention: a study on oats-derived nanoparticles. *Nat. Prod Res.* 13, 1–7. doi: 10.1080/14786419.2025.2477225

Anusuya, S., and Sathiyabama, M. (2014). Preparation of β-D-glucan nanoparticles and its antifungal activity. *Int. J. Biol. Macromol.* 70, 440–443. doi: 10.1016/j.ijbiomac.2014.07.011

Aranjuelo, I., Pérez, P., Hernández, L., Irigoyen, J. J., Zita, G., Martínez-Carrasco, R., et al. (2005). The response of nodulated alfalfa to water supply, temperature and elevated CO2: photosynthetic downregulation. *Physiologia Plantarum* 123, 348–358. doi: 10.1111/j.1399-3054.2005.00459.x

Arruda, S. C., Silva, A. L., Galazzi, R. M., Azevedo, R. A., and Arruda, M. A. (2015). Nanoparticles applied to plant science: a review. *Talanta.* 131, 693–705. doi: 10.1016/j.talanta.2014.08.050

Ashok Kumar, D., Palanichamy, V., and Selvaraj, M. P. (2014). Green aynthesis of silver nanoparticles using Alternanthera dentate leaf extract at room temperature and

their antimicrobial activity. Spectrochem. *Acta Part A Mol. Biomol. Spectrosc.* 127, 168–171. doi: 10.1016/j.saa.2014.02.058

Ashraf, Z. U., Shah, A., Gani, A., Gani, A., Masoodi, F. A., and Noor, N. (2021). Nanoreduction as a technology to exploit ß-Glucan from cereal and fungal sources for enhancing its nutraceutical potential. *Carbohydr Polym.* 258, 117664. doi: 10.1016/j.carbpol.2021.117664

Avellan, A., Schwab, F., Masion, A., Chaurand, P., Borschneck, D., Vidal, V., et al. (2017). Nanoparticle uptake in plants: gold nanomaterial localized in roots of arabidopsis thaliana by X-ray computed nanotomography and hyperspectral imaging. *Environ. Sci. Technol.* 51, 8682–8691. doi: 10.1021/acs.est.7b01133

Bacha, U., Nasir, M., Iqbal, S., and Anjum, A. A. (2017). Nutraceutical, anti-inflammatory and immune modulatory effects of β-glocan isolated from yeast. *Bio. Med. Res. Int.* 2017, 1–14. doi: 10.1155/2017/8972678

Bradford, M. M. (1976). A rapid and sensitive method for the quantitation of microgram quantities of protein utilizing the principle of protein-dye binding. *Anal. Biochem.* 72, 248–254. doi: 10.1016/0003-2697(76)90527-3

Camilli, G., Tabouret, G., and Quintin, J. (2018). The complexity of fungal β-glucan in health and disease: effects on the mononuclear phagocyte system. *Front. Immunol.* 9. doi: 10.3389/fimmu.2018.00673

Chakrapani, K., Chanu, W. T., Sinha, B., Thangjam, B., Hasan, W., Devi, K. S., et al. (2023). Deciphering growth abilities of *fusarium oxysporum f.* sp. *pisi* under variable temperature, pH and nitrogen. *Front. Microbiol.* 14. doi: 10.3389/fmicb.2023.1228442

Chandra, S., Chakraborty, N., and Dasgupta, A. (2015). Chitosan nanoparticles: A positive modulator of innate immune responses in plants. *Sci. Rep.* 5, 15195. doi: 10.1038/srep15195

Chavanke, S. N., Penna, S., and Dalvi, S. G. (2022). -Glucan and its nanocomposites in sustainable agriculture and environment: an overview of mechanisms and applications. *Environ. Sci. pollut. Res. Int.* 29, 80062–80087. doi: 10.1007/s11356-022-20938-z

Chen, G., Liu, Y., Svirskis, D., Li, H., Ying, M., Lu, W., et al. (2024). Cryo-milled β-glucan nanoparticles for oral drug delivery. *Pharmaceutics* 16, 546. doi: 10.3390/pharmaceutics16040546

Chichiriccò, G., and Poma, A. (2015). Penetration and toxicity of nanomaterials in higher plants. *Nanomaterials (Basel)* 5, 851–873. doi: 10.3390/nano5020851

El-Aswad, A. F., Aly, M. I., Alsahaty, S. A., and Basyony, A. B. A. (2023). Efficacy evaluation of some fumigants against Fusarium oxysporum and enhancement of tomato growth as elicitor-induced defense responses. *Sci. Rep.* 13, 2479. doi: 10.1038/s41598-023-29033-w

Elnagar, S. E., Tayel, A. A., Elguindy, N. M., Al-saggaf, M. S., and Moussa, S. H. (2021). Innovative biosynthesis of silver nanoparticles using yeast glucan nanopolymer and their potentiality as antibacterial composite. *J. Basic Microbiol.* 61, 677–685. doi: 10.1002/jobm.202100195

El-Temsah, Y. S., and Joner, E. J. (2012). Impact of Fe and Ag nanoparticles on seed germination and differences in bioavailability during exposure in aqueous suspension and soil. *Environ. Toxicol.* 27, 42–49. doi: 10.1002/tox.20610

Erika, C., Griebel, S., Naumann, M., and Pawelzik, E. (2020). Biodiversity in tomatoes: is it reflected in nutrient density and nutritional yields under organic outdoor production? *Front. Plant Sci.* 11. doi: 10.3389/fpls.2020.589692

Fernández, V., and Eichert, T. (2009). Uptake of hydrophilic solutes through plant leaves: current state of knowledge and perspectives of foliar fertilization. *Crit. Rev. Plant Sci.* 28, 36–68. doi: 10.1080/07352680902743069

Fuertes-Rabanal, M., Largo-Gosens, A., Fischer, A., Munzert K.S. Carrasco-López, C., Sánchez-Vallet, A., Engelsdorf, T., et al. (2024). Linear β-1,2-glucans trigger immune hallmarks and enhance disease resistance in plants. *J. Exp. Bot.* 75, 7337–7350. doi: 10.1093/jxb/erae368

Gao, F., Hong, F., Liu, C., Zheng, L., Su, M., and Wu, X. (2006). Mechanism of nano-anatase TiO2 on promoting photosynthetic carbon reaction of spinach: Inducing complex of Rubisco-Rubisco activase. *Biol. Trace Element Res.* 111, 239–253. doi: 10.1385/BTER:111:1:239

Goncalves, M. F. M., Gomes, S. I. L., Scott-Fordsmand, J. J., and Amorim, M. J. B. (2017). Shorter lifetime of a soil invertebrate species when exposed to copper oxide nanoparticles in a full lifespan exposure test. *Sci. Rep.* 7, 1355. doi: 10.1038/s41598-017-01507-8

Henningen, J. N., Bahamonde, H. A., Mühling, K. H., and Fernández, V. (2023). Tomato and pepper leaf parts contribute differently to the absorption of foliar-applied potassium dihydrogen phosphate. *Plants (Basel).* 12, 2152. doi: 10.3390/plants12112152

Huang, J., Wu, C., Tang, S., Zhou, P., Deng, J., Zhang, Z., et al. (2020). Chiral active β-glucan nanoparticles for synergistic delivery of doxorubicin and immune potentiation. *Int. J. Nanomedicine* 15, 5083–5095. doi: 10.2147/IJN.S258145

Iavicoli, I., Leso, V., Beezhold, D. H., and Shvedova, A. A. (2017). Nanotechnology in agriculture: Opportunities, toxicological implications, and occupational risks. *Toxicol. Appl. Pharmacol.* 329, 96–111. doi: 10.1016/j.taap.2017.05.025

Jangir, M., Sharma, S., and Sharma, S. (2021). Development of next-generation formulation against Fusarium oxysporum and unraveling bioactive antifungal metabolites of biocontrol agents. *Sci. Rep.* 11, 22895. doi: 10.1038/s41598-021-02284-1

Kamiński, K., Hąc-Wydro, K., Skóra, M., Tymecka, M., and Obłoza, M. (2022). Preliminary studies on the mechanism of antifungal activity of new cationic β-glucan derivatives obtained from oats and barley. *ACS Omega* 7, 40333–40343. doi: 10.1021/acsomega.2c05311

Kaziem, A. E., Yang, L., Lin, Y., Xu, H., and Zhang, Z. (2022). β-glucan-functionalized mesoporous silica nanoparticles for smart control of fungicide release and translocation in plants. *ACS Omega* 7, 14807–14819. doi: 10.1021/acsomega.2c00269

Khlebtsov, B. N., and Khlebtsov, N. G. (2011). On the measurement of gold nanoparticle sizes by the dynamic light scattering method. *Colloid J.* 73, 118–127. doi: 10.1134/S1061933X11010078

Kim, Y. T., Kim, E. H., Cheong, C., Williams, D. L., Kim, C. W., and Lim, S. T. (2000). Structural Characterization of ß-d-(1→3, 1→6)-linked glucans using NMR spectroscopy. *Carbohydr. Res.* 328, 331–341. doi: 10.1016/S0008-6215(00)00105-1

Limberger-Bayer, V. M., De Francisco, A., Chan, A., Oro, T., Ogliari, P. J., and Barreto, P. L. M. (2014). Barley β-glucans extraction and partial characterization. *Food Chem.* 154, 84–89. doi: 10.1016/j.foodchem.2013.12.104

Mahmoud, S. H., and Yassein, S. N. (2024). Characterization of β-glucan obtained from Candida albicans of caprine mastitis. *Open Vet. J.* 14, 1269–1280. doi: 10.5455/OVJ.2024.v14.i5.22

Makino, A. (2003). Rubisco and nitrogen relationships in rice: Leaf photosynthesis and plant growth. *Soil Sci. Plant Nutr.* 49, 319–327. doi: 10.1080/00380768.2003.10410016

Manikandan, A., and Sathiyabama, M. (2016). Preparation of Chitosan nanoparticles and its effect on detached rice leaves infected with *Pyricularia grisea*. *Int. J. Biol. Macromolecules* 84, 58–61. doi: 10.1016/j.ijbiomac.2015.11.083

Melo, P. C., Collela, C. F., Sousa, T., Pacheco, D., Cotas, J., Gonçalves, A. M. M., et al. (2020). (Seaweed-based products and mushroom β-glucan as tomato plant immunological inducers. *Vaccines (Basel)* 8, 524. doi: 10.3390/vaccines8030524

Murphy, E. J., Rezoagli, E., Pogue, R., Simonassi-Paiva, B., Abidin, I. I. Z., Fehrenbach, G. W., et al. (2022). Immunomodulatory activity of β-glucan polysaccharides isolated from different species of mushroom—A potential treatment for inflammatory lung conditions. *Sci. Total Environ.* 809, 152177. doi: 10.1016/j.scitotenv.2021.152177

Parthasarathy, R., Chandrika,, Yashavantha Rao, H. C., Kamalraj, S., Jayabaskaran, C., and Pugazhendhi, A. (2020). Molecular profiling of marine endophytic fungi from green algae: Assessment of antibacterial and anticancer activities. *Process Biochem.* 96, 11–20. doi: 10.1016/j.procbio.2020.05.012

Parthasarathy, R., Kumar, S. P., Yashavantha Rao, H. C., and Jayabasakran, J. (2021). Synthesis of β-glucan nanoparticles from red algae-derived β-glucan for potential biomedical applications. *Appl. Biochem. Biotechnol.* 193, 3983–3995. doi: 10.1007/s12010-021-03674-x

Parthasarathy, R., Jayabaskaran, C., Manikandan, A., and Anusuya, S. (2023). Synthesis of nickel-chitosan nanoparticles for controlling blast diseases in asian rice. *Appl Biochem Biotechnol.* 195, 2134–2148. doi: 10.1007/s12010-022-04198-8

Perdomo, J. A., Capó-Bauçà, S., Carmo-Silva, E., and Galmés, J. (2017). Rubisco and rubisco activase play an important role in the biochemical limitations of photosynthesis in rice, wheat, and maize under high temperature and water deficit. *Front. Plant Sci.* 8. doi: 10.3389/fpls.2017.00490

Piani, L., and Papo, A. (2013). Sodium tripolyphosphate and polyphosphate as dispersing agents for alumina suspensions: rheological characterization. *J. Engineering.* 4, 930832. doi: 10.1155/2013/930832

Quinet, M., Angosto, T., Yuste-Lisbona, F. J., Blanchard-Gros, R., Bigot, S., Martinez, J. P., et al. (2019). Tomato fruit development and metabolism. *Front. Plant Sci.* 10. doi: 10.3389/fpls.2019.01554

Riseh, R. S., Vazvani, M. G., and Kennedy, J. F. (2023). β-glucan-induced disease resistance in plants: A review. *Int. J. Biol. Macromol.* 253, 127043. doi: 10.1016/j.ijbiomac.2023.127043

Sathiyabama, M., and Charles, R. E. (2015). Fungal cell wall polymer-based nanoparticles in protection of tomato plants from wilt disease caused by *Fusarium oxysporum f.sp. lycopersici*. *Carbohydr. Polym.* 133, 400–407. doi: 10.1016/j.carbpol.2015.07.066

Seif, S., Sorooshzadeh, A. H., Rezazadeh, S., and Naghdibadi, H. A. (2011). Effect of nano silver and silver nitrate on seed yield of borage. *J. Med. Plant Res.* 5, 171–175. doi: 10.5897/JMPR.9000486

Shang, Y., Hasan, M. K., Ahammed, G. J., Li, M., Yin, H., and Zhou, J. (2019). Applications of nanotechnology in plant growth and crop protection: A review. *Molecules* 24, 2558. doi: 10.3390/molecules24142558

Simonin, M., Richaume, A., Guyonnet, J. P., Dubost, A., Martins, J. M. F., and Pommier, T. (2016). Titanium dioxide nanoparticles strongly impact soil microbial function by afecting archaeal nitriiers. *Sci. Rep.* 6, 33643. doi: 10.1038/srep33643

Stepanova, A. N., Yun, J., Likhacheva, A. V., and Alonso, J. M. (2007). Multilevel interactions between ethylene and auxin in Arabidopsis roots. *Plant Cell.* 19, 2169–2185. doi: 10.1105/tpc.107.052068

Su, Y., Ashworth, V., Kim, C., Adeleye, A. S., Rolshausen, P., Roper, C., et al. (2019). Delivery, uptake, fate, and transport of engineered nanopar-ticles in plants: a critical review and data analysis. *Environ. Sci. Nano* 6, 2311–2331. doi: 10.1039/C9EN00461K

Sundararajan, N., Habeebsheriff, H. S., Dhanabalan, K., Cong, V. H., Wong, L. S., Rajamani, R., et al. (2023). Mitigating global challenges: harnessing green synthesized nanomaterials for sustainable crop production systems. *Glob Chall.* 8, 2300187. doi: 10.1002/gch2.202300187

Tabita, F. R., Hanson, T. E., Li, H., Satagopan, S., Singh, J., and Chan, S. (2007). Function, structure, and evolution of the RubisCO-like proteins and their RubisCO homologs. *Microbiol. Mol. Biol. Rev.* 71, 576–599. doi: 10.1128/MMBR.00015-07

Tan, W. M., Hou, N., Pang, S., Zhu, X. F., Li, Z. H., Wen, L. X., et al. (2012) Improved biological effects of uniconazole using porous hollow silica nanoparticles as carriers. *Pest Manag Sci.* 68, 437–443. doi: 10.1002/ps.2288

Verma, S. K., Das, A. K., Patel, M. K., Shah, A., Kumar, V., and Gantait, S. (2018). Engineered nanomaterials for plant growth and development: A perspective analysis. *Sci. Total Environ.* 630, 1413–1435. doi: 10.1016/j.scitotenv.2018.02.313

Wu, Y., Yang, W., Wang, C., Hu, J., and Fu, S. (2005). Chitosan nanoparticles as a novel delivery system for ammonium glycyrrhizinate. *Int. J. Pharmaceutics* 295, 235–245. doi: 10.1016/j.ijpharm.2005.01.042

Zhao, X., Meng, Z., Wang, Y., Chen, W., Sun, C., Cui, B., et al. (2017). Pollen magnetofection for genetic modification with magnetic nanoparticles as gene carriers. *Nat. Plants.* 3, 956–964. doi: 10.1038/s41477-017-0063-z